MR evaluation of neurovascular lesions after endovascular occlusion with detachable balloons.

E S Kwan, S M Wolpert, R M Scott and V Runge

AJNR Am J Neuroradiol 1988, 9 (3) 523-531
http://www.ajnr.org/content/9/3/523

MR Evaluation of Neurovascular Lesions After Endovascular Occlusion with Detachable Balloons

Eddie S. K. Kwan[1]
Samuel M. Wolpert[1]
R. Michael Scott[2]
Val Runge[1]

Three patients with surgically inaccessible giant carotid aneurysms/pseudoaneurysms and one patient with carotid cavernous fistula had endovascular occlusion with detachable silicone balloons filled with Cholografin. MR was performed before the procedures in three cases and again 18 hr to 44 days after embolization in all four cases. The age-related changes of arterial thrombi, as well as the optimal timing and value of different pulse sequences in the noninvasive follow-up, were evaluated. Arterial thrombi have some characteristics in common with intracerebral hematomas, being isointense on T1-weighted spin-echo images during acute phase and subsequently acquiring hyperintense signals on both T1- and T2-weighted spin-echo images during the subacute and chronic phases. Additional observations are that (1) hyperacute (less than 24 hr old) thrombus is hyperintense on T2-weighted spin-echo sequences; (2) hemosiderin is less conspicuous in chronic intraluminal thrombi than in intracerebral hematomas of comparable size; and (3) thrombosis is initiated at a site remote from the apex of the aneurysm and then progresses centripetally. The Cholografin-filled balloon is hypointense to gray matter on T1-weighted spin-echo images and isointense to both hyperacute and chronic thrombus on T2-weighted spin-echo images. The optimal timing and sequence for MR follow-up of a thrombosed aneurysm with conventional spin-echo technique is beyond 7 days on T1-weighted spin-echo images. The in vivo appearance of Cholografin-filled silicone balloons does not change appreciably on T1- and T2-weighted spin-echo sequences up to 6 weeks if filled according to the manufacturer's specification.

The ability of MR to image stagnant and flowing blood in intracranial hematoma, dural sinus thrombosis, and giant aneurysm has been reported previously [1–7]; however, the age-related changes of arterial thrombi have not been evaluated extensively. Recently, we treated three patients with surgically inaccessible giant carotid aneurysm/pseudoaneurysm and one patient with carotid cavernous fistula by endovascular occlusion with detachable miniballoons filled with Cholografin. Because MR is noninvasive and can image structures beyond the patent vascular lumen, we performed scans before the procedures and again 18 hr to 44 days after embolization with the intention of evaluating (1) the in vivo appearance of acute, subacute, and chronic arterial thrombosis; and (2) the optimal timing for MR and the value of different pulse sequences in the noninvasive follow-up of giant aneurysms treated by endovascular occlusion.

Received May 22, 1987; accepted after revision November 24, 1987.

[1] Department of Radiology, New England Medical Center Hospital, Boston, MA 02111. Address reprint requests to E. S. K. Kwan.

[2] Department of Neurosurgery, New England Medical Center Hospital, Boston, MA 02111.

AJNR 9:523–531, May/June 1988
0195–6108/88/0903–0523

Subjects and Methods

MR imaging was performed on a 1.0-T Siemens system. Multislice, multiecho spin-echo (SE) techniques were routinely used to obtain images on a 25-cm head coil with short repetition time (TR) of 600–800 and echo time (TE) of 17–30, and with long TR of 2.5 to 3 sec and TE of 70–120. Images were acquired on a 256 × 256 matrix for T1-weighted SE sequences. Rectangular pixel matrix with 256 steps in the read-out gradient and 128 steps in the phase-encoding gradient were used for T2-weighted SE images. The raw data were then reconstructed using a two-dimensional Fourier transform technique. The section thick-

ness varied from 5 mm with 1-mm interslice gap to 10 mm with no interslice gap. Axial gradient-refocusing images with a flip angle of 40°, TR = 40, and TE = 12 were also obtained in two cases. All four patients underwent selective carotid and/or vertebral angiography before and after balloon occlusion. The detachable balloon system* was filled with a solution of one part Cholografin 52% and one part sterile water. The MR findings were correlated with angiography and/or clinical signs.

Case Reports

Case 1

A 38-year-old man presented with a 1-month history of right-sided retroorbital headache, ptosis, and hypalgesia in all three divisions of the trigeminal nerve. Cerebral angiography demonstrated a giant right cavernous carotid aneurysm (Fig. 1A), which, with simultaneous compression of the right carotid, also filled from the left internal carotid injection. Owing to the aneurysm's location and the absence of a definable neck, the right distal cervical internal carotid artery was occluded with a detachable balloon.

Follow-up angiography performed ½ hr after the occlusion demonstrated nonfilling of the aneurysm by injections of the right external carotid artery, the left internal carotid artery, and the left vertebral artery. MR images were obtained 24 hr before and 48 hr after occlusion of the distal right cervical internal carotid artery (Figs. 1B–1E). A gradient-refocused image at 48 hr after balloon occlusion confirmed the cessation of flow within the aneurysm (Fig. 1F). The retroorbital headache decreased significantly after balloon embolization, and the patient refused further follow-up MR.

Case 2

A 26-year-old male construction worker sustained blunt neck trauma 6 weeks before admission. He presented with a 4-week history of a pulsatile painful right neck mass, right Horner syndrome, headaches, and right-sided palsies in cranial nerves X and XII. Selective right carotid angiography demonstrated a pseudoaneurysm originating from the distal right cervical internal carotid artery (Figs. 2A and 2B). Because of the increasing mass effect and the anatomic location, an interventional procedure was requested. The first balloon was detached at the neck of the pseudoaneurysm with the intention of preserving flow within the parent vessel. This balloon remained at the neck for approximately 30 sec, after which it was propelled into the apex of the pseudoaneurysm. The second and third balloons were then detached in the right internal carotid artery just proximal to the neck of the pseudoaneurysm. Angiography performed ½ hr after embolization demonstrated nonfilling of the pseudoaneurysm after injections of the right common carotid artery and the left internal carotid artery. MR images were obtained 48 hr before balloon detachment and 18 hr, 7 days, and 44 days after embolization (Figs. 2C–2N). Twenty-four hours after balloon occlusion, the headache and right-sided palsy in cranial nerve X were improved. By the 44th day, the headache, right neck mass, and dysphagia had all disappeared; but the right-sided Horner syndrome and mild hoarseness persisted.

Case 3

A 55-year-old woman presented with a 1½-year history of right hemicranial/retroorbital pain but no cranial nerve dysfunction. Contrast-enhanced CT and selective angiography demonstrated a giant right cavernous carotid aneurysm with no mural thrombus. After an uneventful 30-min trial occlusion of the right internal carotid artery under systemic heparinization, two 2-mm balloons were detached endovascularly. The distal balloon was at the level of the petrous carotid while the proximal balloon was at the C1 level. A follow-up selective left vertebral angiogram demonstrated a minimal amount of stagnant contrast layering along the dependent portion of the giant aneurysm. The patient developed transient horizontal diplopia on the fourth day after embolization. Follow-up MR images were obtained 24 hr, 13 days, and 44 days subsequent to balloon occlusion (Figs. 3A–3F). The patient was totally asymptomatic by the time of the last MR image.

Case 4

A 21-year-old woman presented with headache, ocular bruits, and right-sided palsies in cranial nerve VI and partially in cranial nerve III after being involved in an automobile accident. A CT scan demonstrated fractures along the roof of the right orbit and the right basisphenoid. Selective right internal caroid angiography demonstrated a carotid cavernous sinus fistula with an associated giant pseudoaneurysm arising from the right cavernous internal carotid artery (Fig. 4A). After five balloons were detached within the pseudoaneurysm, selective injection of the right internal carotid artery demonstrated decreased arteriovenous shunting with improved intracranial perfusion (Fig. 4B). The patient noticed a decrease in the ocular bruits and headache; however, the right-sided palsy in cranial nerve VI persisted. Forty days after balloon embolization, the ocular bruits and headache had totally disappeared and the right-sided palsy in cranial nerve VI was improving. MR images were obtained 24 hr before embolization, and both 48 hr and 40 days after embolization (Figs. 4C–4G). The patient refused a follow-up angiogram at the time of the last MR.

Discussion

It is well recognized that the MR appearance of an intracerebral hematoma when imaged with a high-field scanner changes with the age of the lesion. Acute hematomas are isointense on T1-weighted SE sequences and markedly hypointense on T2-weighted SE sequences because of preferential T2 proton relaxation by deoxyhemoglobin within intact red blood cells. Subacute hematomas acquire hyperintense signals on T1- and then T2-weighted SE images sequentially, owing to the formation of paramagnetic methemoglobin from deoxyhemoglobin. With subsequent red blood cell lysis, extracellular methemoglobin results in shortening of T1 relaxation time and prolongation of T2 relaxation time. Chronic hematomas have a hypointense rim both on T1- and T2-weighted SE images, and this rim is more conspicuous on the T2 images due to the markedly shortened T2 of intracellular iron within hemosiderin-laden macrophages. The central hyperintense signal in chronic hematoma is again due to extracellular methemoglobin [2]. There are, however, conflicting opinions in the literature as to the variation in the MR appearances of venous thrombosis over time. Macchi et al. [3] reported the absence of flow void and the presence of collateral venous channels on T1-weighted SE images as the earliest findings. The evolution of the venous thrombi then closely paralleled that of intracerebral hematomas, culminat-

* Bard-Parker, Becton Dickinson & Co., Lincoln Park, NJ 07035.

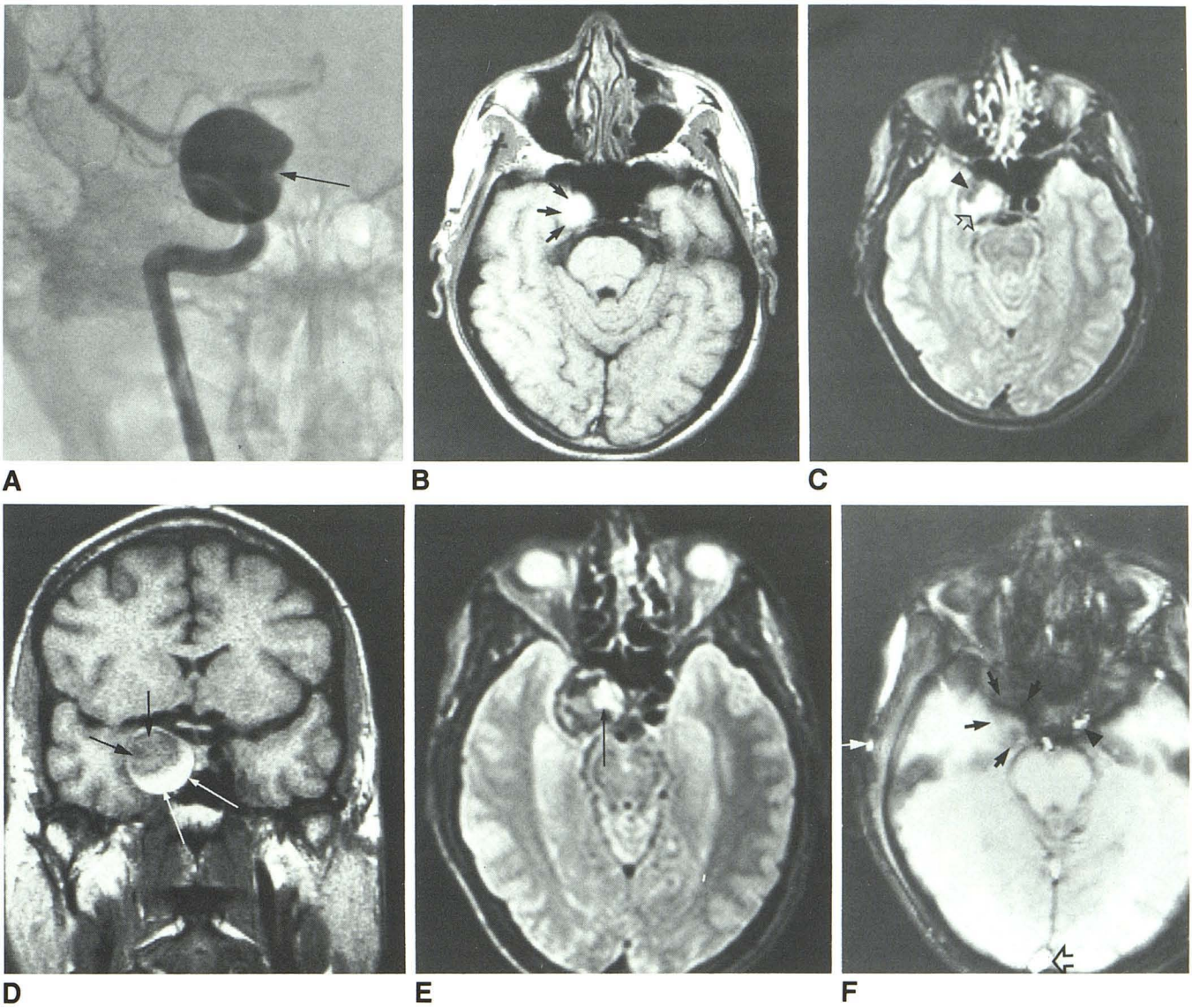

Fig. 1.—*A*, Anteroposterior view of right internal carotid angiogram shows giant cavernous carotid aneurysm. Contour defect (*arrow*) along its medial and inferior wall represents mural thrombus.

***B*, 24 hr before occlusion, axial T1-weighted spin-echo image (800/17) demonstrates hyperintense mural thrombus (*arrows*) along inferior aspect of giant aneurysm.**

***C*, 24 hr before occlusion, axial T2-weighted spin-echo image (3000/70) illustrates mixed hypointense (*arrowhead*) and hyperintense (*open arrow*) mural thrombi. Note absence of hemosiderin along periphery of aneurysm.**

***D*, 48 hr after occlusion of right internal carotid artery, coronal T1-weighted spin-echo image (800/17) shows central region of isointense to gray matter (*black arrows*) corresponding to acute thrombosis. Peripheral high-intensity rim (*white arrows*) lying medial and inferior represents subacute or chronic mural thrombus.**

***E*, 48 hr after balloon occlusion, axial T2-weighted spin-echo image (3000/70) again demonstrates high-intensity mural thrombus (*arrow*) and absence of hemosiderin. Acute thrombosis located laterally contains mixed signals that are both hypo- and isointense to gray matter.**

***F*, 48 hr after balloon occlusion, gradient-refocused image (40/12) demonstrates mixed signals within giant aneurysm (*black arrows*). High-intensity signals compatible with flowing blood are, however, noted within scalp vessels (*white arrows*), left internal carotid artery (*arrowhead*), basilar artery, and torcula (*open arrow*).**

ing in recanalization of the involved venous channels and reappearance of the flow void. In the paper by Macchi et al. [3], the MR images were obtained on a 1.5-T imager from 48 hr to 9 days after the onset of symptoms. Dural sinus thrombosis in the six patients reported by McMurdo et al. [4] demonstrated high intensity signal on all SE sequences (i.e., first and second echo of both short TR and long TR sequences) imaged on either a 0.35-T or a 0.5-T unit from 1 week to 3 months after the initial symptoms appeared. Recent serial in vivo MR studies of human venous thrombi at 0.35-T as reported by Erdman et al. [5] have demonstrated a relatively constant signal characteristic over a 4-week period.

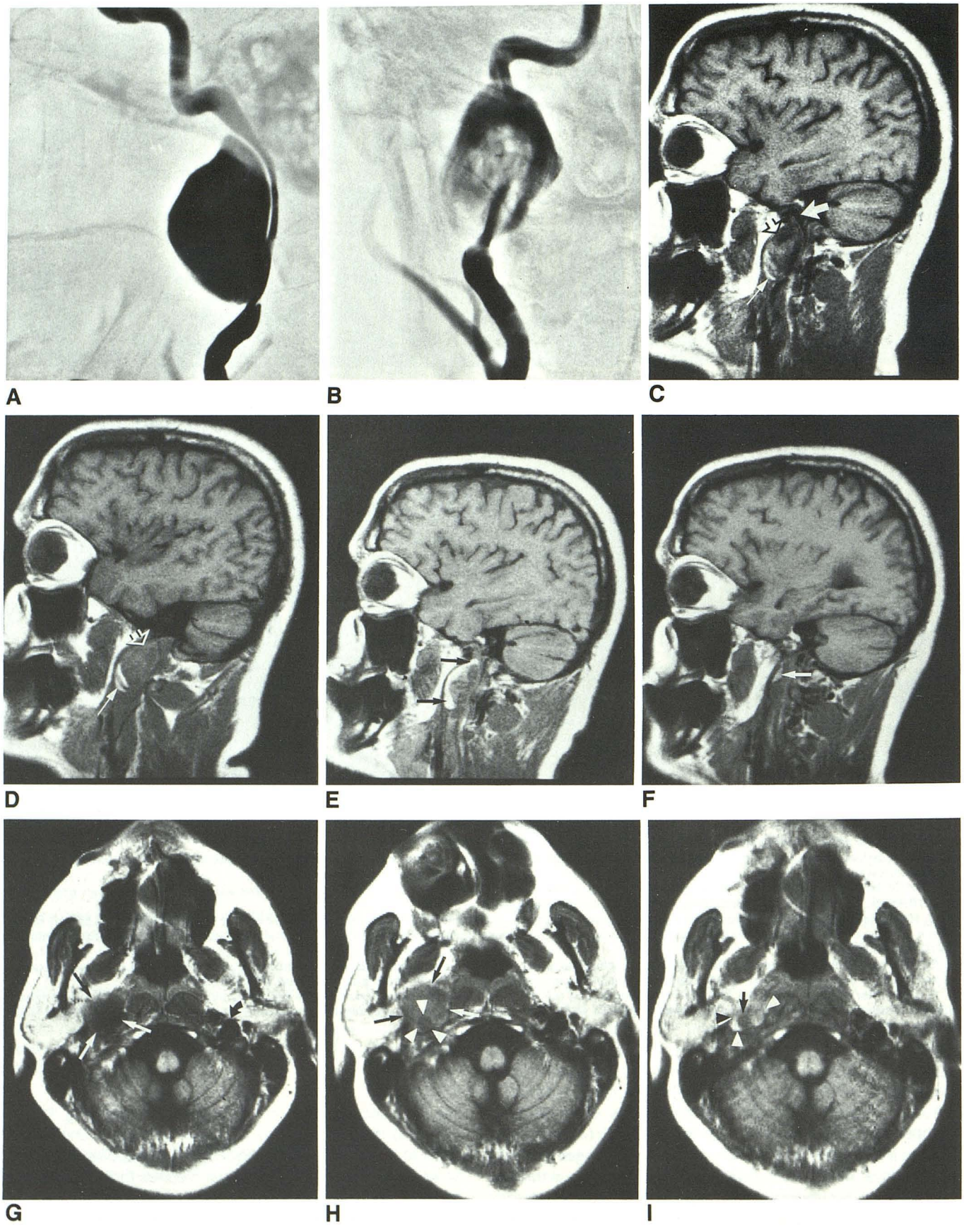
A
B
C
D
E
F
G
H
I

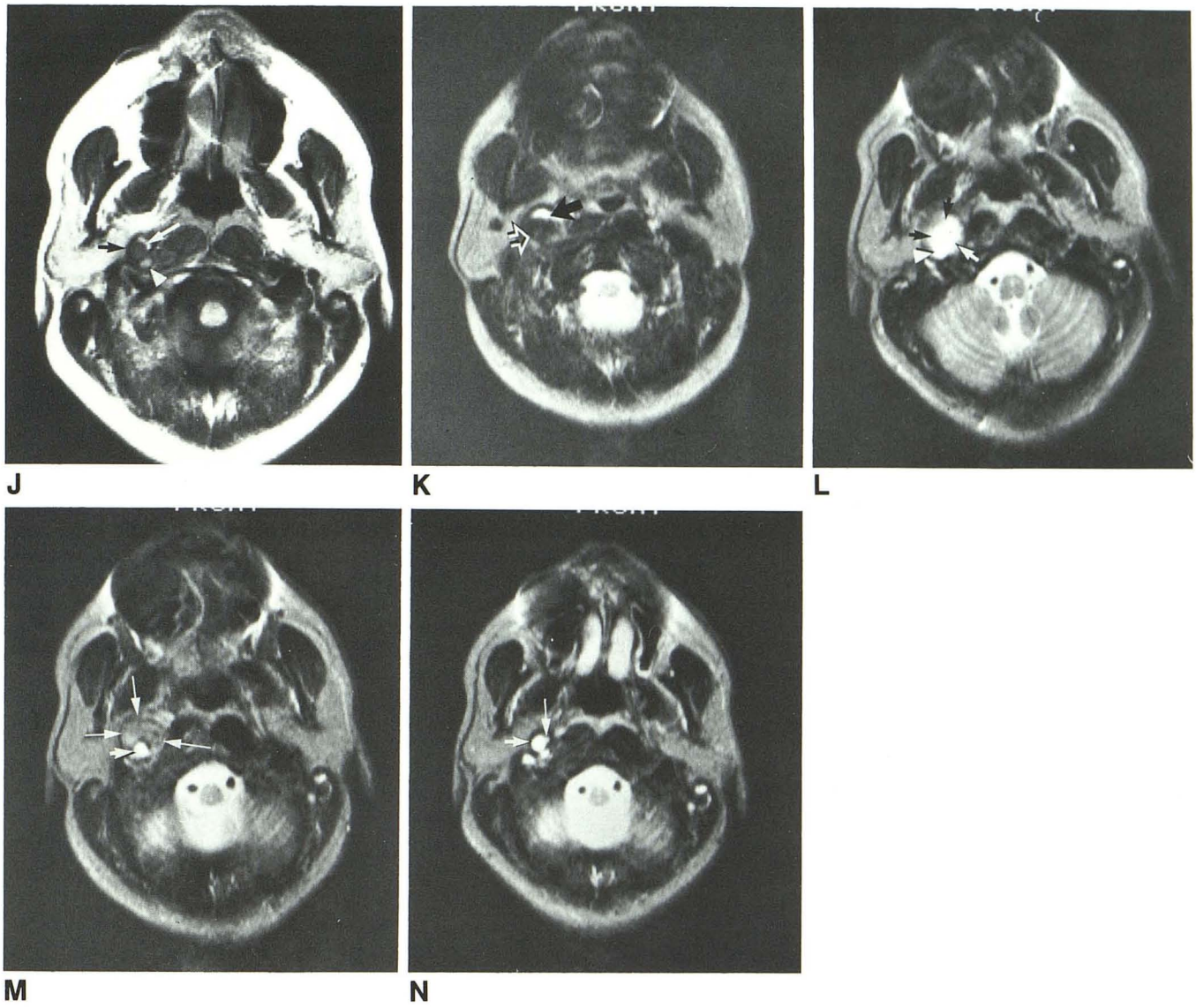

Fig. 2.—Pseudoaneurysm of distal cervical internal carotid artery with compromise of residual lumen.

***A* and *B*, Lateral (*A*) and frontal (*B*) views. Turbulent flow directed from neck toward apex of aneurysm is evident on early arterial phase (*B*).**

***C–F*, Sagittal T1-weighted spin-echo images (600/17) through parapharyngeal space. *C*, 48 hr before occlusion mural thrombus is initially identified along anterior and inferior aspect of aneurysm as high-intensity signals (*small white arrow*). Turbulent flow within apex of aneurysm (*open arrow*) has mixed signal characteristic. Note residual lumen of carotid artery (*large white arrow*). *D*, 18 hr after balloon occlusion multilayered characteristic of mural thrombus (*closed arrow*) is illustrated more clearly. Acute thrombosis within aneurysm (*open arrow*) is both iso- and hyperintense to gray matter. In this particular case, turbulence and acute thrombosis are not easily differentiated on T1-weighted spin-echo image alone. *E*, 7 days after balloon occlusion overall dimension of aneurysm (*arrows*) has decreased, thrombosis has progressed more cephalad toward apex (*top arrow*). *F*, 44 days after balloon occlusion hyperintense pseudoaneurysm (*arrow*) is now collapsed.**

***G–J*, Axial T1-weighted spin-echo images (600/17) through pseudoaneurysm. *G*, 48 hr before balloon occlusion aneurysm (*straight arrows*) is hypointense to gray matter but not as hypointense as contralateral patent jugular vein (*curved arrow*). *H*, 18 hr after balloon occlusion Cholografin-filled balloon (*arrowheads*) is slightly hypointense to acute thrombus within occluded aneurysm (*arrows*). *I*, 7 days after balloon occlusion subacute thrombus (*arrowheads*) is now hyperintense relative to balloon (*arrow*). *J*, 44 days after balloon occlusion a thin rim of low signal intensity presumably representing adventitia is noted along lateral aspect (*black arrow*) of collapsed pseudoaneurysm while a thicker rim of high-intensity signal (*white arrow*) probably representing methemoglobin is located medial to balloon. Thrombosed internal carotid artery (*arrowhead*) is posterior to pseudoaneurysm.**

***K–N*, Axial T2-weighted spin-echo images (2500/120) through pseudoaneurysm. *K*, 48 hr before occlusion hyperintense mural thrombus is present along anterior inferior aspect of pseudoaneurysm (*closed arrow*) while turbulent flow (*open arrow*) is noted posteriorly. *L*, 18 hr after balloon occlusion hyperacute thrombus has high-intensity signal (*arrows*) and is isointense to balloon (*arrowhead*). *M*, 7 days after balloon occlusion thrombus progresses to mixed intensity (*long arrows*). Balloon (*short arrow*) is now hyperintense to thrombus. *N*, 44 days after balloon occlusion chronic thrombosis (*long arrow*) cannot be distinguished from Cholografin-filled balloon (*short arrow*) in this sequence.**

Owing to the nonspecific presenting symptoms in a majority of cases, the onset of spontaneous venous thrombosis is difficult to document precisely.

Patients undergoing endovascular occlusion of giant aneurysm provided us with a unique opportunity to document accurately the onset of thrombosis and the serial in vivo appearance of this process. Thrombi that arise in the rapidly moving arterial or cardiac circulation are composed largely of

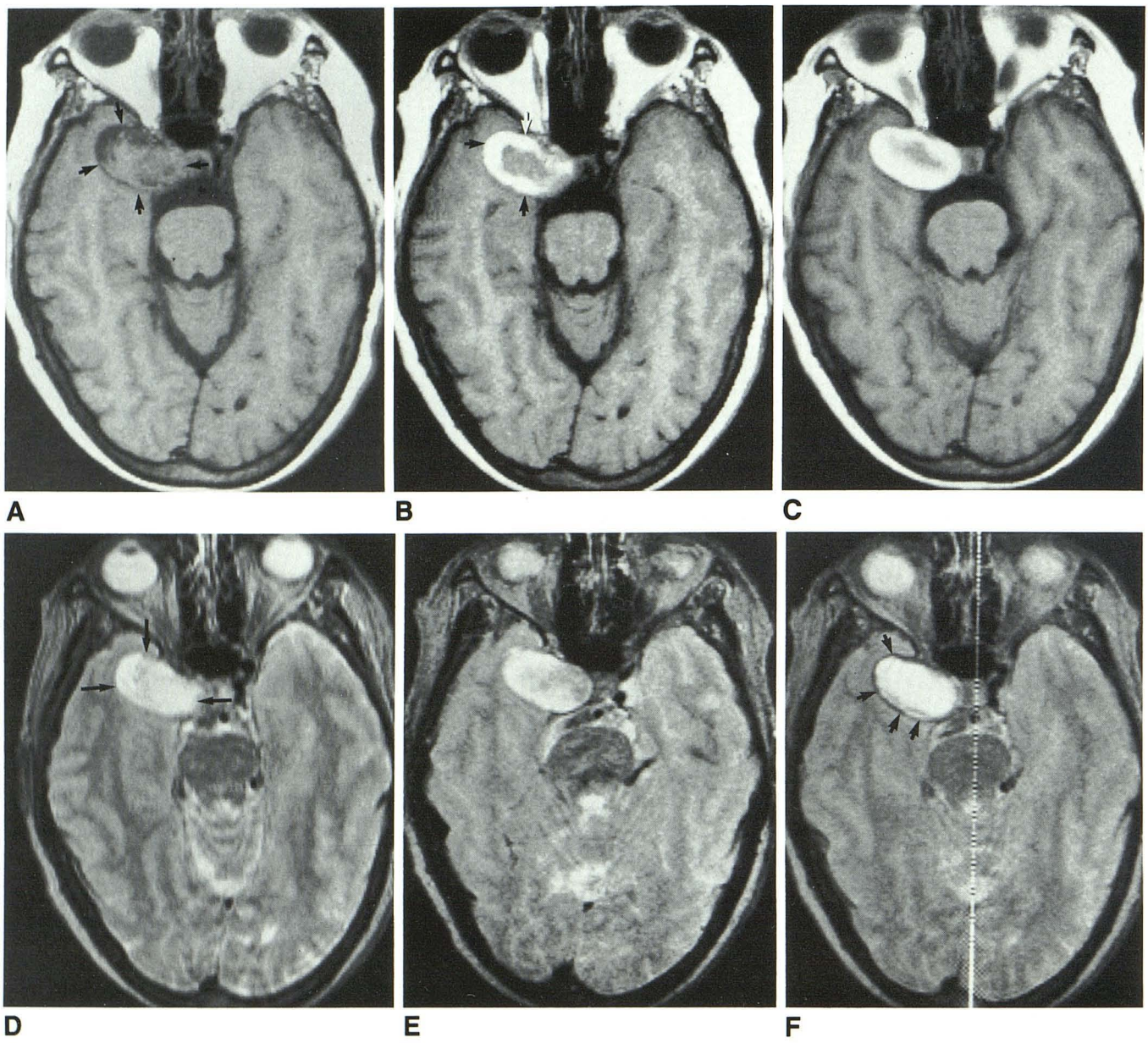

Fig. 3.—*A–C*, Axial T1-weighted spin-echo images (600/17) through giant right cavernous carotid aneurysm. *A*, 24 hr after balloon occlusion, acute thrombus within aneurysm (*arrows*) has both hypo- and isointense signals. *B*, 13 days after balloon occlusion, subacute thrombus now demonstrates peripheral hyperintense rim (*arrows*) and isointense center. *C*, 44 days after balloon occlusion, there is further filling of central isointense zone with hyperintense chronic thrombus.

***D–F*, Axial T2-weighted spin-echo images (3000/70) through same region. *D*, 24 hr after balloon occlusion, predominantly hyperintense signals are noted within acutely thrombosed giant aneurysm (*arrows*). *E*, 13 days after occlusion, subacute thrombus has mixed iso- and hyperintense signals. *F*, 44 days after occlusion, chronic thrombus is again hyperintense. A thin rim of hypointensity is noted peripherally (*arrows*).**

fibrin and platelets with only a few trapped red and white blood cells, and thus usually bear little resemblance to a hematoma grossly [8]. However, with very sluggish arterial or venous flow, there is an increase in the number of red and white blood cells, and thrombi may closely resemble hematomas. As thrombi undergo organization, variable histologic appearances ranging from extensive fibrosis with granulation tissue to relatively unstructured thrombus can be encountered. Thrombi produced iatrogenically by proximal arterial occlusion, as in the four patients in this report, have some characteristics in common with intracerebral hematomas on a high-field MR imager; however, significant differences were observed during the hyperacute and chronic phases (Table 1).

In both patient 1 and patient 2, mural thrombi that were present before proximal carotid occlusion were hyperintense on both T1- and T2-weighted MR images, thus closely paralleling the appearance of subacute or chronic hematomas. The only difference in these cases is the absence of hypointense hemosiderin within or surrounding the mural thrombi.

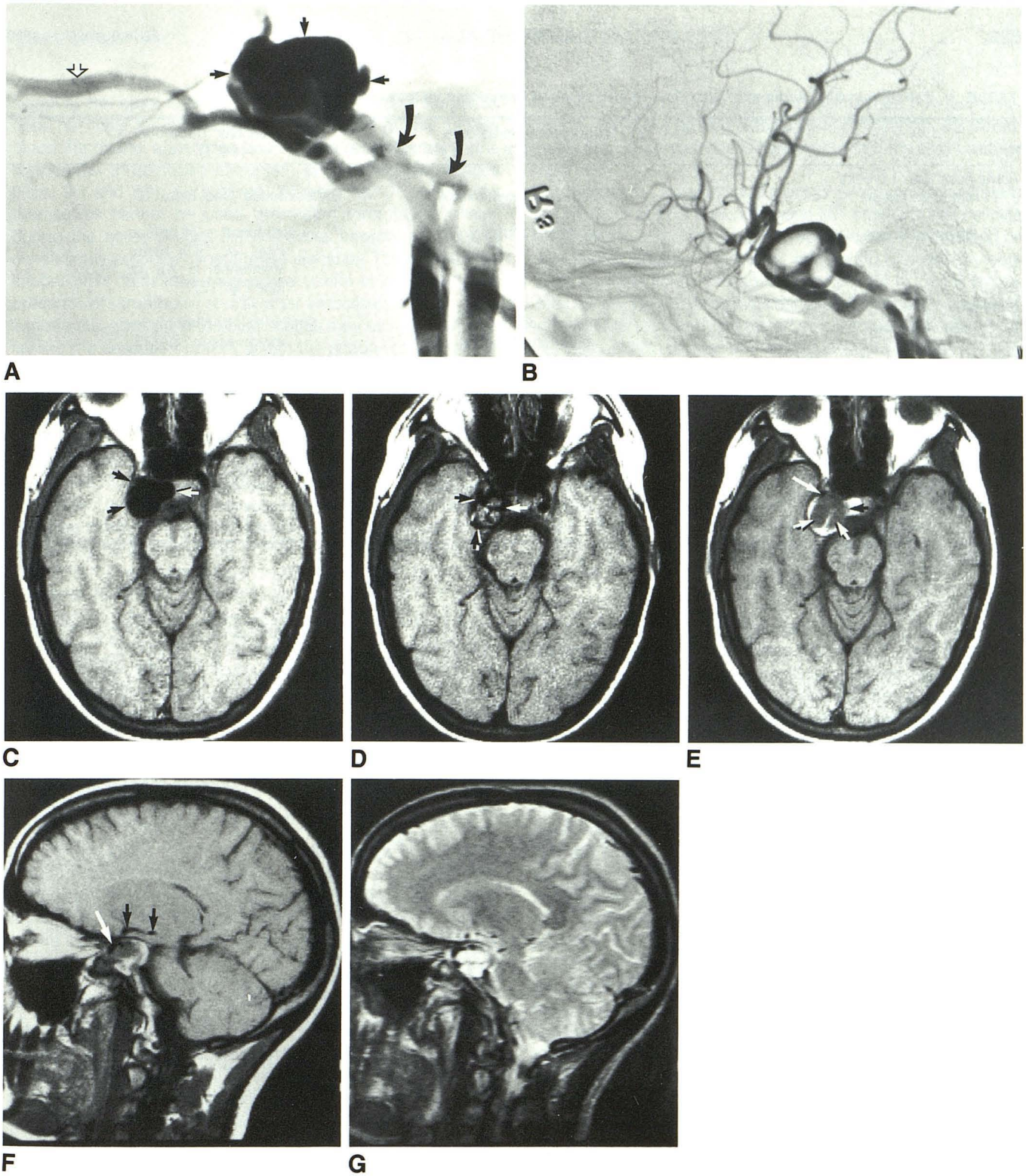

Fig. 4.—*A*, Lateral view of right internal carotid angiogram shows carotid cavernous fistula with associated giant pseudoaneurysm (*straight arrows*). Note rapid shunting to superior ophthalmic vein (*open arrow*) and inferior petrosal sinuses (*curved arrows*).

***B*, Lateral view of right internal carotid injection after detachment of five balloons within giant pseudoaneurysm. The arteriovenous shunting has decreased and intracranial flow has improved, but the fistula is still partially open.**

***C–E*, Axial T1-weighted spin-echo images (600/17) through giant pseudoaneurysm. *C*, 24 hr before balloon occlusion flow void (*arrows*) is noted within pseudoaneurysm. Medial aspect of pseudoaneurysm herniates into sella turcica. *D*, 48 hr after balloon occlusion scattered regions of high intensity compatible with either slow flow or acute thrombosis are interspersed between Cholografin-filled balloons, which are slightly hypointense to gray matter. Flow void is still detected along periphery of pseudoaneurysm (*arrows*). *E*, 40 days after balloon occlusion high-intensity signal compatible with chronic thrombi surrounds balloons (*short arrows*); residual cavernous carotid artery is still patent (*long arrow*).**

***F*, 40 days after balloon occlusion sagittal T1-weighted spin-echo image (600/17) through pseudoaneurysm shows preservation of flow in distal cavernous internal carotid artery (*long arrow*) and middle cerebral artery branch (*short arrows*).**

***G*, Sagittal T2-weighted spin-echo image (3000/70) through same level and on same day as *F*. Chronic thrombosis and Cholografin-filled balloons cannot be separated in this sequence, as both have hyperintense signals. Note absence of hypointense hemosiderin within chronic thrombi.**

TABLE 1: Variation in Signal Intensity with Time in Intracerebral Hematoma vs Intravascular Thrombus

	Intracerebral Hematoma (1.5 T)[a]	Intravascular Thrombus (1.0 T)
Acute (less than 1 week)		
T1-weighted image	Isointense/ hypointense	Isointense (see Figs. 1D, 2H)
T2-weighted image	Hypointense centrally	Hyperintense ≤ 24 hr (see Figs. 2L, 3D); hypo/ isointense ≥ 48 hr (see Fig. 1E)
Subacute (1 week–1 month)		
T1-weighted image	Isointense centrally, hyperintense peripherally	Similar to intracerebral hematoma (see Figs. 2E, 2I, 3B)
T2-weighted image	Hypointense centrally, hyperintense peripherally	Mixed iso/hyperintense (see Figs. 2M, 3E)
Chronic (more than 1 month)		
T1-weighted image	Hyperintense	Hyperintense (see Figs. 2J, 3C, 4E)
T2-weighted image	Hyperintense with markedly hypointense rim	Hyperintense with/without hypointense rim (see Figs. 2N, 3F, 4G)

[a] From [2].

In both cases, thrombus was initiated below the neck of the aneurysm (Figs. 1D and 2C) and then progressed toward the apex and centripetally. This phenomenon was due to the turbulent jet stream directed at the apex and relative stasis below the aneurysm neck. In patient 2, the MR study obtained within 18 hr of occlusion of the internal carotid artery demonstrated hyperintense signals within the pseudoaneurysm on T2-weighted SE images (Fig. 2L). This finding was not due to partial volume effects of the peripheral chronic mural thrombus, as an identical finding was apparent on adjacent slices. This hyperintense signal of "hyperacute" (less than 24 hr old) thrombus is contrary to the usual published description of acute hematoma, but it has previously been reported in intracerebral hematoma of a rhesus monkey model by Di Chiro et al. [9] on the same day after an injection of blood into the monkey's brain. Few studies have been published on hyperacute (less than 24 hr old) intracerebral hematoma in humans. Olsen et al. [10] have experimentally demonstrated intermediate T1 and long T2 characteristics in nonflowing, nonthrombosed human intravascular blood. In vitro results from Yuasa and Kundel [11] likewise confirmed T2 of rabbit blood to be significantly longer than that of fat and muscle. During the hyperacute stage, we postulate that the hyperintense signal within the thrombosed aneurysm is due to the intrinsic long T2 characteristic of intravascular oxyhemoglobin prior to its conversion to deoxyhemoglobin. As a result, the preferential T2 proton relaxation enhancement effect of deoxyhemoglobin in intact red blood cells (i.e., marked hypointense signal on T2-weighted SE images) is not manifested in the hyperacute thrombosed aneurysm. Slow flow within the aneurysm can potentially mimic the appearance of hyperacute thrombus on T2-weighted SE images, but this can be excluded on the basis of hyperintense signal in both the first and second echo of the T2-weighted SE image and the nonfilling of the pseudoaneurysm from all possible potential sources of collaterals on angiography. As a rule, flow-related enhancement is less evident on T2-weighted SE images because as TR is lengthened there is greater recovery of the proton magnetization in the soft tissue adjacent to the vessel. This results in less signal differential between the intravascular and extravascular compartments. In patient 2 a combined isointense and hyperintense signal was seen within the thrombosed aneurysm 7 days later; but at 44 days, the thrombus was all hyperintense. The hyperintense signal of intravascular thrombus at 44 days is due to the prolongation of T2 in the presence of extracellular methemoglobin after complete red blood cell lysis. The mixed intensity of subacute thrombus is due to an interplay of the opposing effects of intracellular deoxyhemoglobin/methemoglobin (both result in low signal on T2-weighted SE images due to preferential T2 proton relaxation enhancement) and extracellular methemoglobin (which results in high signal on T2-weighted SE images due to simultaneous shortening of T1 and prolongation of T2) as the red blood cells undergo lysis. The conversion of intracellular deoxyhemoglobin to methemoglobin precedes red blood cell lysis. The rapid shrinkage of thrombus within the pseudoaneurysm in patient 2, as seen in Figure 2F, is in keeping with the natural history of carotid artery dissection and subsequent thrombus lysis, organization, and incorporation in the vessel wall. The rapid dissolution of blood elements outside the CNS as exemplified by this patient perhaps accounts for the conspicuous absence of hemosiderin deposit on T2-weighted SE images. Similar findings have previously been reported by Goldberg et al. [12] in the follow-up MR of one of their patients 7 weeks after a cervical carotid dissection.

A potential pitfall in the assessment of the patency of an aneurysm is also demonstrated in patient 2. On T1-weighted SE images, turbulent flow within the aneurysm has an intermediate to hypointense signal (Fig. 2C). In general, the signal intensity will vary with the degree of turbulence. Although the

signal at the apex is lower than the rest of the aneurysm it does not have the characteristic flow void of rapidly moving blood. Its overall apperance bears some resemblance to the hyperacute thrombosed aneurysm on T1-weighted images (Figs. 2C and 2D). As a result, T1-weighted SE images by themselves cannot be used to confirm thrombosis reliably during the acute phase. If hyperacute thrombi turn out to consistently produce hyperintense signal on T2-weighted SE images, this technique may prove useful in confirming the presence of thrombosis shortly after embolization. With more experience, gradient-refocused images may be helpful in confirming the cessation of flow within the aneurysm, as seen in patient 1.

The Cholografin-filled balloon is slightly hypointense to gray matter on T1-weighted SE images, whereas acute thrombosis is isointense to gray matter on these images. This lack of contrast makes separation of the balloons from acute thrombosis difficult on T1-weighted SE sequences. The Cholografin-filled balloon on T2-weighted SE images, however, is isotense relative to hyperacute and chronic thrombosis, but can barely be distinguished from a 7-day-old thrombus (Fig. 2M). From our limited experience, the optimal timing and sequence for MR follow-up of thrombosed aneurysms/fistulae is beyond 7 days on T1-weighted SE sequences when a subacute thrombus turns hyperintense and the balloon remains slightly hypointense to gray matter. T1-weighted SE images are preferable to T2-weighted SE images because of the shorter scanning time, better signal-to-noise ratio, and better contrast between balloon and acute thrombus. Even though the silicone balloons are semipermeable, their appearance does not change appreciably on either the T1- or T2-weighted SE sequences up to 6 weeks if filled according to the manufacturer's specification.

After an incomplete closure of the carotid cavernous fistula with associated pseudoaneurysm in patient 4, serial MR provided the opportunity to follow this patient noninvasively. Unfortunately, the patient refused angiography at the time of the last MR, and we do not have angiographic proof that the cavernous carotid fistula is indeed completely closed. However, the cessation of orbital bruits, the gradual improvement of the palsy in cranial nerve VI, and the MR findings provide reasonable evidence that the fistula and the giant pseudoaneurysm are indeed thrombosed.

Among all surgically inaccessible giant intracranial aneurysms treated with carotid ligation, approximately 30–50% [13, 14] will not fill on postoperative angiography. In the past it could only be inferred that the aneurysms were thrombosed; however, a small percentage of them did not fill either because of vasospasm or because of small collaterals. Serial MR is an ideal imaging technique for understanding the pathophysiology of these aneurysms after proximal carotid ligation/occlusion. It is also well known that a carotid-cavernous fistula can often thrombose spontaneously after an incomplete closure with a detachable balloon [15]. MR would again be an excellent method by which to demonstrate this process noninvasively. In the future, increased experience with flow-sensitive pulse sequences—such as phase-sensitive SE technique or gradient-refocused imaging in which the flip angle, TR, and TE have been optimally adjusted to maximize flow enhancement—will make MR more accurate in predicting acute thrombosis (Fig. 1F) in vascular lesions treated via the endovascular approach.

In summary, intravascular thrombi produced iatrogenically by proximal arterial occlusion have MR characteristics similar to subacute and chronic intracerebral hematoma obtained on a high-field imager. In addition, our limited experiences suggest (1) hyperacute thrombus (less than 24 hr old) is hyperintense on T2-weighted SE images, a finding that is at variance with previously reported acute intracerebral hematomas: (2) hemosiderin is less conspicuous in chronic intraluminal thrombi than in intracerebral hematomas of comparable size; (3) turbulence within a giant aneurysm may in certain instances be difficult to distinguish from a hyperacute thrombosed aneurysm on T1-weighted SE images; and (4) the optimal timing and sequence for follow-up of an iatrogenically thrombosed aneurysm is beyond 7 days on T1-weighted SE images. Additional experience with gradient-refocused images may enable MR to be more accurate in predicting thrombosis during the hyperacute or acute stages after intravascular intervention.

REFERENCES

1. Bradley WG, Waluch V. Blood flow: magnetic resonance imaging. *Radiology* **1985**;154:443–450
2. Gomori JM, Grossman RI, Goldberg HI, Zimmerman RA, Bilaniuk LT. Intracranial hematomas: imaging by high field MR. *Radiology* **1985**;157:87–93
3. Macchi PJ, Grossman RI, Gomori JM, Goldberg HI, Zimmerman RA, Bilaniuk LT. High field MR imaging of cerebral venous thrombosis. *J Comput Assist Tomogr* **1986**;10:10–15
4. McMurdo SK, Brant-Zawadzki M, Bradley WG, Chang GY, Berg BO. Dural sinus thrombosis: study using intermediate field strength MR imaging. *Radiology* **1986**;161:83–86
5. Erdman WA, Weinreb JC, Cohen JM, Buja LM, Chaney C, Peshock RM. Venous thrombosis: clinical and experimental MR imaging. *Radiology* **1986**;161:233–238
6. Atlas SW, Grossman RI, Goldberg HI, Hackney DB, Bilaniuk LT, Zimmerman RA. Partially thrombosed giant intracranial aneurysms: correlation of MR and pathologic findings. *Radiology* **1987**;162:111–114
7. Olsen WL, Brant-Zawadzki M, Hodes J, Norman D, Newton TH. Giant intracranial aneurysms: MR imaging. *Radiology* **1987**;163:431–435
8. Baumgartner HR. The role of blood flow in platelet adhesian, fibrin deposition and formation of mural thrombi. *Microvasc Res* **1973**;5:167–179
9. DiChiro G, Brooks RA, Girton ME, et al. Sequential MR studies of intracerebral hematomas in monkeys. *AJNR* **1986**;7:193–199
10. Olsen WL, Kucharczyk W, Keyes WD, Norman D, Newton TH. Magnetic resonance characterization of non-flowing intravascular blood. *Acta Radiol [Diagn]* (Stockh) **1986**;369:63–66
11. Yuasa Y, Kundel HL. Magnetic resonance imaging following unilateral occlusion of the renal circulation in rabbits. *Radiology* **1985**;154:151–156
12. Goldberg HI, Grossman RI, Gomori JM, Ashbury AK, Bilaniuk LT, Zimmerman RA. Cervical internal carotid dissecting hemorrhage. Diagnosis using MR. *Radiology* **1986**;158:157–161
13. Pool JL, Potts DG. *Aneurysms and arterio-venous anomalies of the brain: diagnosis and treatment*. New York: Harper & Row, **1965**:463
14. Giannotta SL, McGillicuddy JE, Kindt GW. Gradual carotid artery occlusion in the treatment of inaccessible internal carotid artery aneurysms. *Neurosurgery* **1979**;5:417–421
15. Tsai FY, Hieshima GB, Mehringer CM, Grinnell V, Pribram HW. Delayed effects in the treatment of carotid-cavernous fistulas. *AJNR* **1983**;4:357–361